

Magnetic and Spectroscopic Investigations on Cobalt-Alumina and Cobalt-Molybdenum-Alumina

Electron Spin Resonance of the Oxidized, Sulfided, and Reduced Catalysts

M. LOJACONO,* J. L. VERBEEK, AND G. C. A. SCHUIT†

Laboratory of Inorganic Chemistry and Catalysis, Eindhoven University of Technology, Eindhoven, The Netherlands

Received November 21, 1972

The ESR spectra of $\text{CoO-Al}_2\text{O}_3$, $\text{MoO}_3\text{-Al}_2\text{O}_3$ and $\text{CoO-MoO}_3\text{-Al}_2\text{O}_3$ were investigated in the oxidized state and after reduction with $\text{H}_2 + \text{H}_2\text{S}$ (sometimes followed by a further treatment with H_2) or by H_2 . All Co-containing samples produce signals at 1200 Oe (for $\gamma\text{-Al}_2\text{O}_3$) which shift to 1750 and 4300 Oe after treatment at 1300°C (formation of $\alpha\text{-Al}_2\text{O}_3$). The signals are assigned to Co^{2+} in tetrahedral sites in the support: they are not affected by sulfiding or reduction. If no Mo is present, reduction leads to the formation of an extremely broad and strong signal ascribed to cobalt metal: it is eliminated by the presence of Mo. In the absence of Co and in the oxidized state Mo-containing samples develop a weak signal at $g = 1.93$, assigned to traces of Mo^{5+} in free MoO_3 ; in the presence of Co this signal disappears. Pretreatment of Mo-containing samples with $\text{H}_2 + \text{H}_2\text{S}$ leads first to a hundredfold enhancement of the signal which, however, disappears after application of longer reduction times or higher temperatures. No signal connected with Mo^{3+} could be found. Finally, H_2 after $\text{H}_2 + \text{H}_2\text{S}$ treatments produced a signal at $g = 2.16$ if Co was present; it is assigned to either Co^+ or Co^{2+} (low spin).

A catalyst model is proposed containing two solid states. State I is the support with Co^{2+} and Mo^{6+} in its subsurface layers. Its fate after reduction is uncertain but Co^{2+} is not changed. State II is a separate system of compounds, Co_3O_4 , MoO_3 or CoMoO_4 depending on the composition. Treatments with $\text{H}_2 + \text{H}_2\text{S}$ lead, respectively, to $\text{Co} + \text{CoS}$, MoS_2 or $\text{CoS} + \text{MoS}_2$ (CoMo_3S_4).

INTRODUCTION

The so-called Co-Mo-alumina catalyst for the hydrodesulfurization of petroleum feedstocks is unquestionably one of the most important industrial catalysts: its mode of action and in particular the role of the promoter Co, are yet insufficiently understood. To understand the catalytic activity, a good knowledge of the catalyst structure appears necessary and a number

of investigations were aimed at obtaining more information in this connection. The older work was mainly directed at the measurement of magnetic susceptibilities because this property can produce information regarding the valency state of the cobalt promoter, i.e., whether it is present as the metal or as Co^{2+} . If the latter was true the paramagnetic susceptibility might show whether it was octahedrally or tetrahedrally surrounded [see Richardson (1), Tomlinson, Keeling, Rymer, and Bridges (2)]. This work usually led to the assignment of a tetrahedral coordination to the Co^{2+} and to the assumption that its state was comparable to that of Co in the spinel

* On leave of absence from Centro di Studio del C.N.R. sulle Strutture ed Attività Catalitica di Sistemi di Ossidi, Institute of General Chemistry, University of Rome, Rome, Italy.

† To whom correspondence should be sent.

CoAl_2O_4 . Later work of Ashley and Mitchell (3) and Lipsch and Schuit (4) in which the magnetic measurements were combined with reflectance spectroscopy in the visible appeared to confirm these results. Information concerning the state of the Mo remained scarce: it is often assumed (4) to be present as a monolayer on the alumina surface. None of this work, however, led to an elucidation of the state of the reduced and/or sulfided catalyst.

We therefore undertook to investigate whether electron spin resonance studies might lead to additional information. At the time this work was started, hardly anything was known about ESR on Co-Mo-alumina catalysts. Some results became known during the investigation but at the time when our results were being processed for publication, a considerable amount of work from elsewhere became available. We mention the work of Seshadri and co-workers (5, 6), of Hagenbach and co-workers (7, 8) and most important of Voorhoeve and Stuiver (9) on the probably related system Ni-W- Al_2O_3 . A comparison of our work with the published information often shows agreement but sometimes also discrepancies.

The present report summarizes our work and compares it with the results of the other workers in the field. Consequent to our work we propose a structural model for the catalyst in the oxidized and sulfided/reduced form.

EXPERIMENTAL

a. Preparation of Samples

The γ -alumina used throughout this investigation was prepared according to the method described by McIver *et al.* (10). X-ray diagrams did not indicate the presence of other phases. Cobalt was incorporated by adding an amount of a solution of $\text{Co}(\text{NO}_3)_2 \cdot 6(\text{H}_2\text{O})$ (Merck p.a.) equal to the pore volume of the solid component. The solution was titrated before impregnation. The solid mass was then dried at 120°C and subsequently fired in air for 24 hr at 600°C . Some samples were fired at 1300°C : the 600°C -fired samples are

further referred to as A- γ -Co- x , the 1300°C -fired samples are A'Co- x , where x denotes the cobalt content as number of Co-atoms per 100 Al atoms. In addition to the samples prepared in this way, a series of cobalt containing samples was also prepared in which the firing at 600°C was omitted: these are referred to as A $^\circ$ - γ -Co- x .

In order to prepare samples containing Mo and Co, Mo was first introduced by impregnation of γ - Al_2O_3 , in a similar way as given above, with a solution of ammonium hepta-molybdate (Merck p.a.), drying at 120°C , grinding and firing in air at 500°C for 24 hr and subsequently adding the Co as described above. The samples were then fired at 600°C in air for 24 hr; they are further referred to as A- γ -MoCo- y , x , where y and x give the nominal Mo and Co content, again as the number of Mo and Co atoms per 100 Al atoms.

b. Pretreatment of the Samples with H_2 or $\text{H}_2 + \text{H}_2\text{S}$

Reduction of the samples, like hydro-sulfidation, was usually carried out for 2 hr at a temperature in the range of 25 – 500°C . Various methods were applied, indicated by A, B, C, or D. They are specified as follows:

(A) The catalyst contained in a silica boat was subjected to a stream of gas in a glass tube, placed in an oven, the temperature of the sample being measured at the position of the boat with a thermocouple. Gas flow $100 \text{ cm}^3\text{min}^{-1}$, gas composition 90% H_2 + 10% H_2S , the flows being measured separately. The samples were allowed to cool in the reducing atmosphere and subsequently exposed to air at room temperature and then transferred to the ESR tubes.

(B) Similar to (A) but contact with air was avoided. To do so the sample tube was sealed into the reduction vessel. After reduction the system was closed via its stopcocks and the sample transferred to the sample tube by turning the assembly upside down. The method allowed subsequent treatments for a single sample.

(C) The sample was given a treatment according to (B) for 2 hr at 400°C . Here-

after it was further reduced with H_2 ($100 \text{ cm}^3\text{min}^{-1}$, 1 atm) at 460°C . Exposure to air was avoided.

(D) The catalyst was reduced with pure H_2 ($100 \text{ cm}^3\text{min}^{-1}$, 1 atm) without pre-treatment by $\text{H}_2 + \text{H}_2\text{S}$.

c. ESR Measurements

Most samples were investigated in the AEG X-band spectrometer with standard rectangular cavity. Field marking was provided by a ruby crystal, permanently mounted in the cavity (in the figures the field markers are indicated by arrows). Fields and scans were calibrated with an AEG NMR-field measuring and regulating system. This system was equipped with a Hewlett & Packard Electronic Counter 5245L, which also served, in combination with a H & P. Frequency Converter, to measure the microwave frequency.

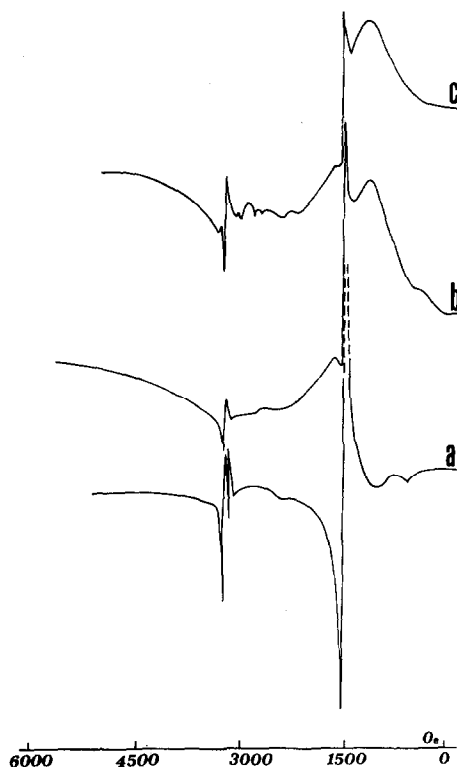


FIG. 1. ESR spectra (Co I) of (a) $\gamma\text{-Al}_2\text{O}_3$, (b) A- $\gamma\text{-Co-2}$, (c) A- $\gamma\text{-MoCo-5:2}$. Final calcination temperature in all cases 600°C . X-ray diagram in all cases $\gamma\text{-Al}_2\text{O}_3$. Numbers give atoms Co and Mo per 100 atoms Al. Gain in all cases the same.

RESULTS

I. Samples Treated with Air Only

Figure 1 gives the ESR spectra at room temperature of (a) $\gamma\text{-Al}_2\text{O}_3$, (b) A- $\gamma\text{-Co-2}$, and (c) A- $\gamma\text{-MoCo-5:2}$, hence all treated at 600°C . It is seen that the $\gamma\text{-Al}_2\text{O}_3$ contains some, so far unidentified, ESR-active impurity. Addition of Co leads to the formation of an extra signal (Co I), a relatively broad signal around 1200 Oe. This signal is also present, and even to a somewhat larger degree, in the Mo-containing sample. The position of Co I was not found to be influenced by the Co concentration. We attempted to measure the

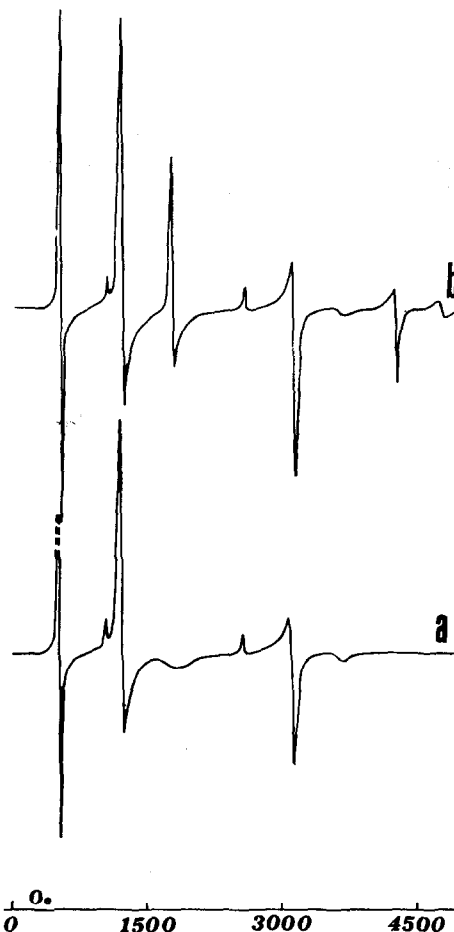


FIG. 2. ESR spectra (Co II) of (a) Al_2O_3 (1300°C), (b) A' Co-1. Final calcination temperature 1300°C . Gain in all cases the same.

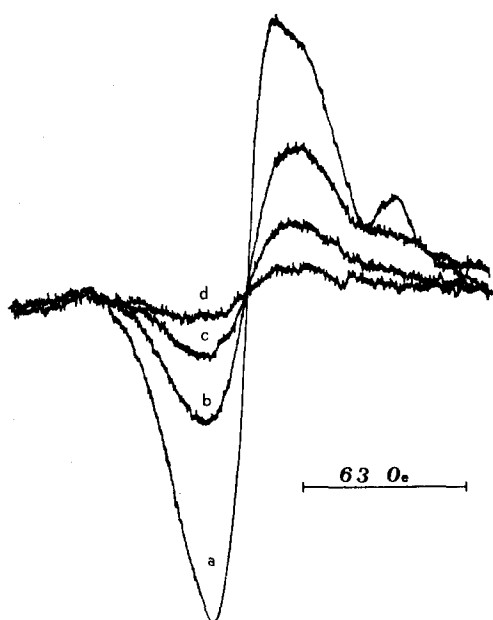


FIG. 3. ESR spectra (Mo I) of (a) A- γ -Mo-5, (b) A- γ -MoCo-5:1, (c) A- γ -MoCo-5:2, (d) A- γ -MoCo-5:5. Final calcination temperatures in all cases 600°C. Gain same for all samples.

ESR spectra at He temperatures (1–4 K) but these experiments failed because the Al_2O_3 then showed a number of extra resonances that made identification of other Co signals impossible. The only point worth mentioning was that the Co I signal was no longer present, perhaps because of antiferromagnetic interaction.

Figure 2 reports the spectra of the alumina and A'Co-I (b) both samples having been pretreated at 1300°C. Again we notice the presence of impurities in the alumina (now presumably α - Al_2O_3) but at a different position. New signals are found after incorporation of Co: their characteristic resonances are at 1750 and 4300 Oe. The combination will be named Co II.

Figure 3 gives the spectra of the molybdenum-containing samples A- γ -Mo:5 and A- γ -MoCo 5: x , all obtained at room temperature. Note the decrease with Co content. The sample containing only Mo shows an extra signal at $g = 1.93$ with low intensity. A similar signal will be described in Mo-containing samples after reduction but then at a much greater intensity (factor

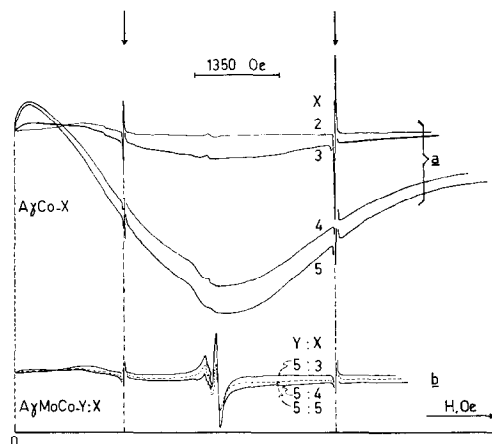


FIG. 4. ESR spectra (Co III) at room temperature of A- γ -Co- x and A- γ -MoCo-5: x after reduction and sulfiding at 400°C for 2 hr (100 ml/min; 1 atm. 90 H_2 + 10 H_2S). (a) A- γ -Co- x ; $x = 2, 3, 4, 5$; (b) A- γ -MoCo-5: x ; $x = 3, 4, 5$. Gain (arbitrary units) = 8. No Co III present if Mo is in excess.

100 stronger). Since it is obviously connected with molybdenum, it will be called Mo I. It is noteworthy that the intensity of Mo I decreases with increasing signal strength of Co I.

II. Reduced and Sulfided Samples

(a) In Figs. 4a and 4b the ESR (room temperature) spectra are given of A- γ -Co- x ($x = 2, 3, 4, 5$) and A- γ -MoCo-5: x ($x = 3, 4, 5$) after a treatment according to A at 400°C for 2 hr. The spectra in Fig. 4a are characterized by the presence of a very broad and strongly asymmetric signal which is very prominent for $x = 4$ and 5, although it is also present, albeit to a much lesser extent, at lower Co concentrations. It is obviously connected with the presence of Co and will therefore be named Co III. When Mo is present (see Fig. 4b) the intensity of this signal is far smaller: even for A- γ -MoCo-5:5 it is hardly observable. The low gain required for an adequate recording of the broad signal prevents obtaining information as to signal Co I. Therefore Fig. 5 shows the region 0–2200 Oe for some samples A- γ -Co- x and A- γ -MoCo-5: x at 12.5 times the gain used in Fig. 4. It becomes evident from this that

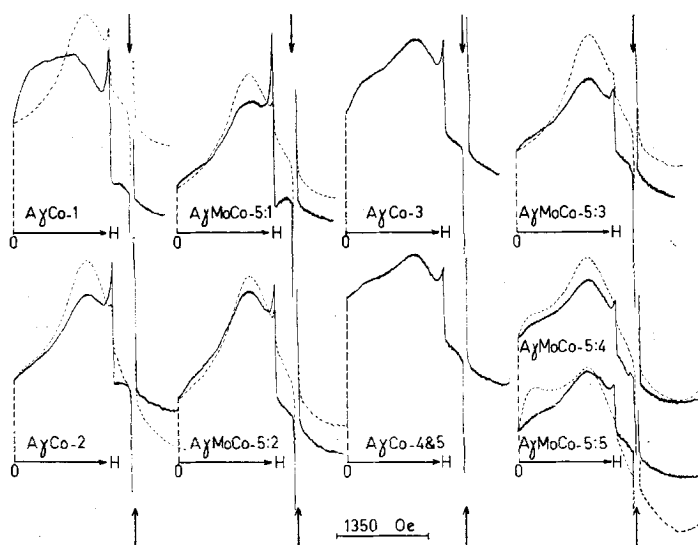


FIG. 5. ESR spectra (Co I) (low-field range) of $A\text{-}\gamma\text{-Co-}x$ and $A\text{-}\gamma\text{-MoCo-}5:x$ at room temperature. Full lines: after calcination in air at 600°C (24 hr). Dotted lines: samples after 2 hr at 400°C in $90\text{ H}_2 + 10\text{ H}_2\text{S}$. Amplification factor = 100 (same unit as Fig. 4).

Co I is still present and even in a slightly higher concentration.

(b) When the samples mentioned under (a) were reduced by method D (pure H_2), the broad signal appeared again but was markedly more intense. For instance, after 2 hr at 400°C , a very broad signal was obtained which spoiled the Q -factor of the cavity, though just not enough to interfere seriously with the measurement. However, after a more prolonged reduction, it proved entirely impossible to tune the cavity. Reduction of a sample $A^\circ\text{Co-}2$ (not fired in air) produced a considerably more intense Co III signal than its pre-fired counterpart $A\text{-}\gamma\text{-Co-}2$. The influence of time and temperature of reduction is illustrated in Fig. 6 for some samples $A\text{-}\gamma\text{-Co-}x$.

(c) Samples $A\text{-}\gamma\text{-Co-}x$ and $A\text{-}\gamma\text{-MoCo-}5:x$ ($x = 1,2,3,4,5$) were next treated according to C. The result is given in Fig. 7a. It is clear that a treatment by H_2 subsequent to one with $\text{H}_2 + \text{H}_2\text{S}$ produces a new signal, "on top" of the broad Co III signal if present. It is obviously connected with Co and will be termed Co IV. Its g value is 2.16. It is also present in $A\text{-}\gamma\text{-MoCo-}5:3$ but its intensity is lower, contrary to what was found by Hagenbach,

Menguy, and Delmon (7) who reported a similar signal for mixtures of Co_9S_8 and MoS_2 with, however, the maximum intensity at a $\text{Co}/(\text{Co} + \text{Mo})$ ratio of 0.2:0.25. In our samples the intensities grew with time and seemed to attain a maximum after

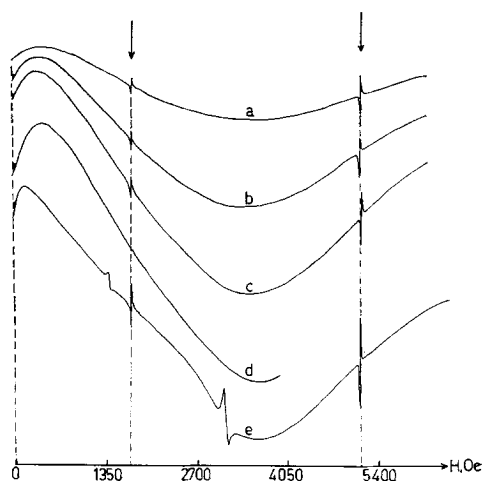


FIG. 6. ESR spectra (Co III) at room temperature after reduction with H_2 of (a) $A\text{-}\gamma\text{-Co-}3$ 2 hr, 400°C H_2 , gain 4; (b) 2 hr, 450°C H_2 , gain 4; (c) 6 hr, 450°C H_2 , gain 4; (d) $A\text{-}\gamma\text{-Co-}5$ 2 hr, 400°C H_2 , gain 1; (e) $A^\circ\text{-}\gamma\text{-Co-}2$ 2 hr, 400°C H_2 , gain 10. Amplification factors in same arbitrary units as Fig. 3.

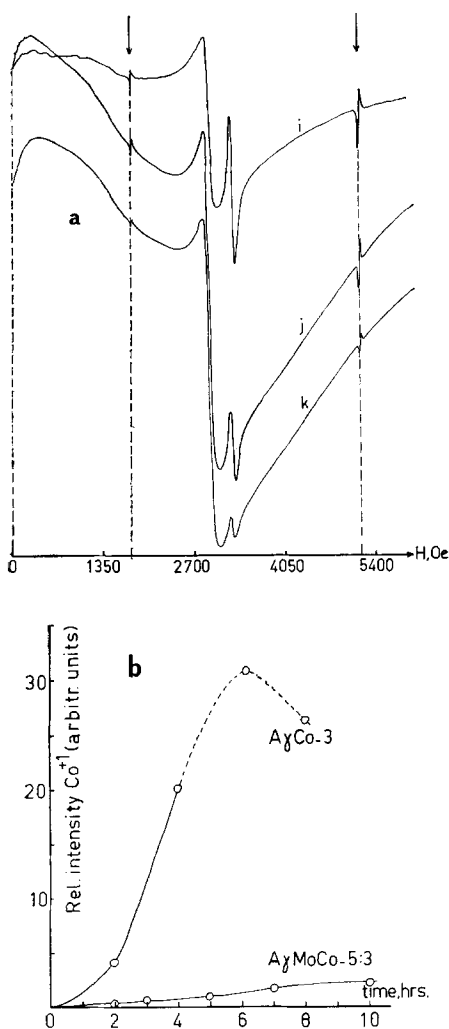


FIG. 7. (a) ESR spectra (Co IV and Mo I) at room temperature of $A\text{-}\gamma\text{-MoCo-5:3}$, presulfided with $90 \text{ H}_2 + 10 \text{ H}_2\text{S}$, followed by reduction with H_2 for: (p) 2 hr at 460°C : gain 8 (units as before); (q) 5 hr at 460°C : gain 5; (r) 10 hr at 460°C : gain 2. (b) Comparison of intensities of Co IV signal as a function of time of reduction (presulfided $90 \text{ H}_2 + 10 \text{ H}_2\text{S}$ 2 hr 400°C , followed by H_2 reduction at 450°C for time stated in figure).

about 6–10 hr (Fig. 7b). Exposure to air destroys the signal, the “broad band” remaining present. Even prolonged evacuation at 500°C failed to restore it but H_2 treatment at 450°C fully recovered it. An attempt to reproduce a similar signal in pure CoS failed because the “broad band” signal was so intense as to make any

measurement impossible, even in tubes with less than 1 mm internal diameter.

(d) Another feature of samples containing Mo is the presence of signal Mo I ($g = 1.93$). A similar signal was found by Masson and Nechtschein (11), Seshadri and Petrakis (5) and Seshadri, Massoth, and Petrakis (6). Figure 8 gives relative intensities in $A\text{-}\gamma\text{-Mo-5}$ and $A\text{-}\gamma\text{-MoCo-5:3}$ as a function of treatment temperature, using method A or B. It follows that oxygen apparently reoxidizes part of the Mo species connected with this signal, at a fairly rapid state, even at ambient temperature.

(e) Finally, Mo-containing samples, treated by method A, exhibited a triple g -value signal centered at $g = 2.04$. We designate it as Signal S. The signal did not appear after application of methods B and D. Similar signals have been reported by Seshadri *et al.* and Dudzik *et al.* (12). They ascribe it to some sulfur species. It will not be discussed further in the present paper, but reserved for another publication

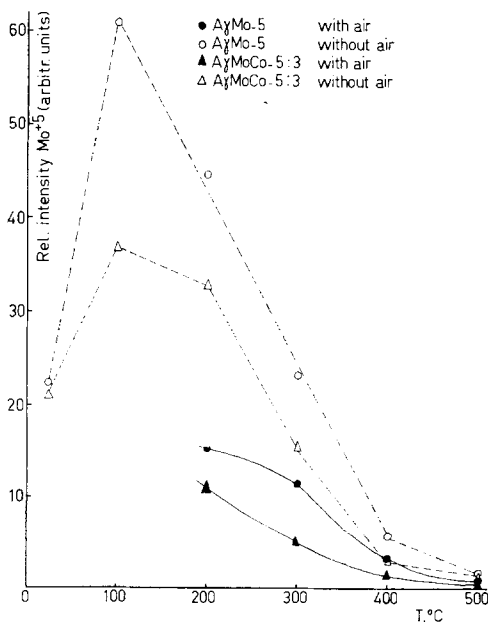


FIG. 8. Influence of the severity of the pretreatment with $90 \text{ H}_2 + 10 \text{ H}_2\text{S}$ on the intensity of the Mo I signal. For $A\text{-}\gamma\text{-Mo-5}$ and $A\text{-}\gamma\text{-MoCo-5:3}$. Samples have been exposed to air after pre-treatment or measured in the absence of air (----- or - - - - -).

TABLE 1
SURVEY OF VARIOUS SIGNALS AFTER DIFFERENT PRETREATMENTS

Sample Pre-treatment	A- γ -Co		A- γ -CoMo			A- γ -Mo	
Air	Co I	Precursor	Co I	S	Mo ⁶⁺ very weak	S	Mo ⁶⁺ weak
H ₂ + H ₂ S	Co I	Co III	Co I	S	Mo ⁶⁺ strong, disappears	S	Mo ⁶⁺ strong disappears later
H ₂ + H ₂ S H ₂	Co I	Co III + Co IV strong	Co I	Co IV weak			
H ₂		Co III very strong					

(13). Table 1 summarizes the data on the signals observed as a function of catalyst composition and pretreatment.

DISCUSSION

We shall start with an attempt to identify the various ESR signals with chemical species, i.e., transition metal-ions or atoms in a certain ligand surrounding.

Co I and Co II

Under the conditions where these signals are produced the most conspicuous cobalt species is Co^{2+} in tetrahedral coordination. Evidence for its presence was derived from reflectance spectroscopy (relatively strong band at 7000 cm^{-1} giving rise to the blue color of the oxidized catalyst) and magnetic measurements [see Richardson (1), Ashley and Mitchell (3), and Lipsch and Schuit (4)]. It is supposed to reside in the support at tetrahedral interstices and to be somewhat similar to Co^{2+} in the spinel CoAl_2O_4 when the sample is not heated in excess of temperatures around 600°C . Treatments by H_2 or $\text{H}_2 + \text{H}_2\text{S}$ do not appear to change either signal position or signal strength in good agreement with the difficult reduction of the spinel. We therefore propose that Co I is connected with Co^{2+} in tetrahedral coordination in $\gamma\text{-Al}_2\text{O}_3$

and consequently Co II in a similar configuration in $\alpha\text{-Al}_2\text{O}_3$.

This assignment is supported by a more detailed analysis of the resonance positions. A comparison of our results on Co^{2+} in alumina with those of van Reijen (14) on Cr^{3+} in alumina shows the existence of a close similarity between the two sets of data. Van Reijen reports broad signals for Cr^{3+} in $\gamma\text{-Al}_2\text{O}_3$ at 1200 Oe and in $\alpha\text{-Al}_2\text{O}_3$ at 1800 and 4300 Oe, hence at almost identical positions as Co I and Co II. To understand this similarity it is advantageous to reproduce van Reijen's theoretical treatment for the origin and position of his signals.

The Cr^{3+} ion has a 4F ground state which is split by an octahedral field into 4A_2 , 4T_2 and 4T_1 , the first being the ground state and 4T_1 the highest excited state in the manifold of d-orbitals. Spin-orbit coupling in combination with distortion of the octahedral symmetry is the cause of the zero-field splitting. Writing the spin Hamiltonian as:

$$g_x H_x S_x + g_y H_y S_y + g_z H_z S_z + D(S_z^2 - 5/4) + E(S_x^2 - S_y^2) \quad (1)$$

where $D = 3D_z/2$ and $E = 1/2(D_x - D_y)$, van Reijen first shows that the Zeeman terms do not contribute appreciably to the zero-field splitting and anisotropy effects,

their contributions being of the order of 1% (i.e., 30 Oe). The terms connected with D and E only contribute to zero-field splitting if they originate from a perturbation that splits the 4T_2 levels, i.e., when the perturbation is derived from a potential

$$P \cdot xy + Q \cdot xz + R \cdot yz \quad (2)$$

If $P = Q = R$ the perturbation is trigonal ($\alpha\text{-Al}_2\text{O}_3$); if only one of them is different from zero, it is orthorhombic ($\gamma\text{-Al}_2\text{O}_3$). If the perturbations are large, for instance when $D \gg h\nu$, the resonances at low fields converge to:

orthorhombic distortion

$$g\beta H/h\nu = 1/(1 + \sqrt{3}) \quad \text{and} \quad E/D = 1/3, \quad (3)$$

hence the resonance occurs at 1200 Oe;

trigonal distortion

$$g\beta H/h\nu = E/2 = 0, \quad (4)$$

resonance at 1700 Oe.

For this particular situation and orthorhombic distortion D becomes:

$$D = 3q\lambda^2/\epsilon_0^2 \quad (5)$$

where q is the energy difference between the 4T_2 levels, λ is the spin-orbit coupling constant, and ϵ_0 is the crystal-field splitting for the unperturbed case.

It should be stressed that the Cr^{3+} signals observed by van Reijen are by no means characteristic for Cr^{3+} signals of octahedral compounds since the zero-field splitting is surprisingly large. Schulz-Dubois (15) was the first one to give an explanation for the special case of ruby (Cr^{3+} in $\alpha\text{-Al}_2\text{O}_3$) and to ascribe it to a strong trigonal distortion of the octahedra presumably due to the distribution of the Al^{3+} ions. Van Reijen then found that for boehmite and its dehydration product such as $\gamma\text{-Al}_2\text{O}_3$ there exists another, orthorhombic, but equally strong distortion. The Cr^{3+} ion therefore acts as a probe for point-group distortions in the aluminas, having their origin in the way the aluminium ions are positioned in the crystal lattice.

Passing now to Co^{2+} we notice that:

(a) If placed in a tetrahedral configura-

tion the orbital arrangements are the same as those of Cr^{3+} in octahedral coordination with, however, the crystal-field splitting, ϵ_0 , being smaller for the tetrahedral case.

(b) Zero-field effects occur because of the distortion of the octahedral and tetrahedral coordination leading to "scrambling" of the 4A_2 and 4T_2 orbitals via spin-orbit interaction. While normally the distortions of the surroundings for Cr^{3+} and Co^{2+} in their compounds are different and consequently the zero-field effects different in quantity and even sign [see Abragam and Bleaney (16)], these distortions are now correlated because the sites belong to the same lattice and are defined by the symmetry properties of that lattice. To illustrate this, Fig. 9 presents the situation of a tetrahedral site which is surrounded by four octahedral sites. If the lattice is distorted from the ideal situation in such a manner that the octahedral sites are subjected to an orthorhombic distortion, a similar distortion should occur for the tetrahedral site. In particular, if this distortion leads to a $P \cdot xy$ perturbation of the crystal-field it should do this for both octahedra and tetrahedra. A necessary consequence of this assumption is that a change in the lattice properties has to change the position of the Co^{2+} and Cr^{3+} signals simultaneously and similarly. Since this is precisely what has been found to be the case in the change from $\gamma\text{-Al}_2\text{O}_3$ to $\alpha\text{-Al}_2\text{O}_3$ we consider this as a proof for the validity of the assumption.

(c) The D for the tetrahedral case is, if anything, greater than for the octahedral case [see Eq. (5)]. The spin-orbit coupling constant λ is greater for Co^{2+} than for Cr^{3+} (it is also of a different sign but this is irrelevant because it occurs as λ^2). The crystal field splitting ϵ_0 is considerably smaller for the tetrahedral situation. Presumably q , the 4T_2 splitting factor, is smaller but the factor q/ϵ_0^2 is almost certainly greater for tetrahedral surroundings, so D (tetrahedral) $>$ D (octahedral). Since D (octahedral) $\gg h\nu$ the exact similarity of the two series of signals is almost required by the conditions.

Our final conclusion, therefore, is that the Co I and Co II signals are connected with

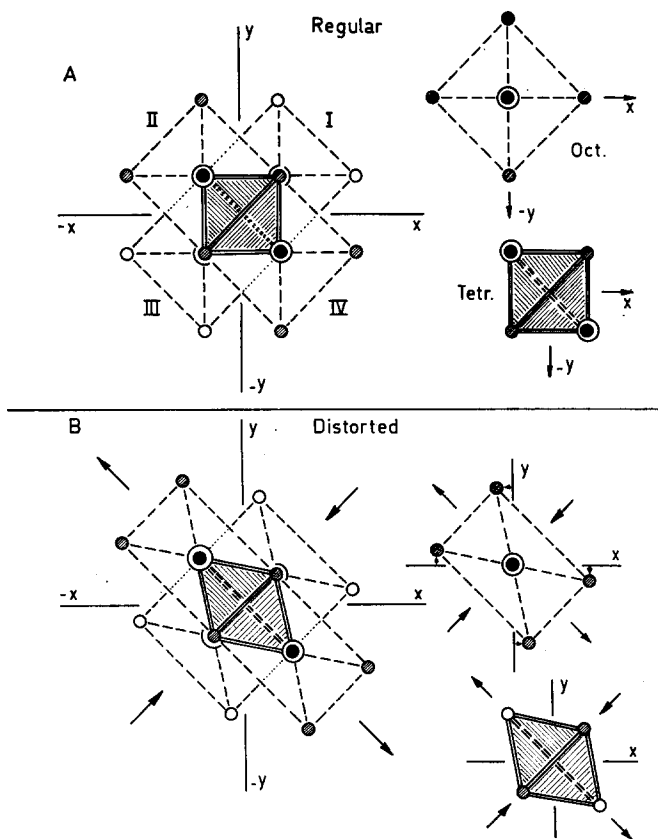


FIG. 9. Projection of system of a tetrahedron with four adjoining octahedra on xy plane and consequences of a crystal-lattice distortion consisting of an elongation along one diagonal and a constriction along the other on the xy plane. Octahedra then become distorted according to an orthorhombic distortion with potential symmetry P_2xy (see van Reijen). A similar distortion occurs for the tetrahedron showing that in the crystal lattice octahedral and tetrahedral distortions are correlated.

the presence of Co^{2+} in a tetrahedral coordination in the alumina support.

It should be noted that the position of the Co^{2+} signals for $\gamma\text{-Al}_2\text{O}_3$ is not that expected for CoAl_2O_4 since a spinel has trigonal distortion of the lattice. This parallels van Reijen's conclusions (14) for Cr^{3+} . Although Co^{2+} in $\gamma\text{-Al}_2\text{O}_3$ is therefore related to Co^{2+} in CoAl_2O_4 , it is not entirely similar.

Co III

The signal is probably connected with the presence of metallic cobalt. Richardson (1) has shown from magnetic measurements that metallic Co can indeed be formed and moreover the circumstances that lead to the formation of a strong Co III signal are those that might be considered

favorable for the production of metallic Co, such as a high Co concentration and the absence of a high-temperature pretreatment of the impregnated sample. On the other hand, reduction with $\text{H}_2 + \text{H}_2\text{S}$ instead of with H_2 leads to a less strong signal, evidently because of the simultaneous formation of Co-sulfide which is more difficult to reduce (see also Richardson). It is interesting that the signal strength increases considerably between $A_7\text{Co-3}$ and $A_7\text{Co-4}$. In the samples with a cobalt content less than 3%, the Co I (Co^{2+} in tetrahedral coordination, presumably in the $\gamma\text{-Al}_2\text{O}_3$) remains observable and as far as could be ascertained, at comparable intensities as in the unreduced state. Therefore, this particular form of Co^{2+} is not accessible to reduction and the Co com-

pound that is the precursor of the metallic cobalt must be a different species. Tomlinson *et al.* (2) concluded from magnetic measurements that Co_3O_4 was present in the nonreduced material and Keeling confirmed the existence of a separate Co_3O_4 phase in alumina from a study of the Cobalt K absorption edge (17). Since Co_3O_4 is undoubtedly reduced by H_2 to the metal and only partially so if treated with $\text{H}_2 + \text{H}_2\text{S}$, the assumption of Co_3O_4 as the precursor of metallic Co and therefore of the signal Co III, appears well founded.

Co IV

The signal is only observed if cobalt is present and if the sample is first reduced with $\text{H}_2 + \text{H}_2\text{S}$ and subsequently with H_2 . It must therefore be connected with some reduced form of CoS or Co-Mo sulfide. A similar signal was reported by Hagenbach, Menguy, and Delmon (7) for mixtures of Co_3S_8 and MoS_2 with maximum signal strength at Co/(Co + Mo) ratios between 0.2–0.25. It is not clear at present which species is responsible for the signal. Locher and Geschwind (18) and Low and Suss (19) report similar signals which they ascribe to Co^{1+} . Van den Berg (20) prepared CoMo_2S_4 and determined its structure from X-ray measurements and its formal valency

from magnetic measurements. The compound has one spin assigned to the low-spin state of Co^{2+} and should therefore be $\text{Co}^{2+}\text{Mo}_2^{3+}\text{S}_4^{2-}$. The trivalent Mo cations are supposed to occur in diamagnetic pairs. According to her, low-spin Co^{2+} ($3d^7$) also occurs in CoS. It is not impossible that such a low spin Co^{2+} would give rise to an ESR signal as reported here and by Hagenbach *et al.*: this might thus be caused either by Co^{1+} or Co^{2+} (low spin).

Mo I

There is hardly any doubt that this signal belongs to Mo^{5+} in a tetragonal square arrangement as also postulated by Seshadri *et al.* and Masson *et al.*

Signal S

This signal was first reported by Seshadri *et al.* who ascribed it to polymeric sulfur radicals.

Having thus formed a set of assignments for the various signals, we shall now attempt to construct models for the catalyst structure in its various stages of preparation and for the reactions that lead to these structures (see Table 2).

Impregnation of $\gamma\text{-Al}_2\text{O}_3$ with Co nitrate followed by drying, seems in the first instance to form Co_3O_4 . If the sample is then heated to higher temperatures Co

TABLE 2
ASSIGNMENTS OF SIGNALS OR PRECURSORS OF SIGNALS

Sample	A- γ -Co		A- γ -CoMo		A- γ -Mo
Air	Co^{2+} (tetr.) in $\gamma\text{-Al}_2\text{O}_3$	Co_3O_4	$\text{Co}^{2+} + \text{Mo}^{6+}$ in $\gamma\text{-Al}_2\text{O}_3$	CoMoO_4	MoO_3 dispersed in pores
$\text{H}_2 + \text{H}_2\text{S}$	id	Co metal + CoS	id (sulfided)	CoS + MoS_2	Mo^{4+}S_2 via Mo^{5+}
$\text{H}_2 + \text{H}_2\text{S}$ H_2	id	id + Co^{1+} or Co^{2+}	id	$\text{Co}^{2+}(\text{Mo}^{3+})_2\text{S}_4^{2-}$ or $\text{Co}_9\text{S}_8 + \text{MoS}_2$	
H_2	id	Co metal			

ions appear to diffuse into the support and to occupy tetrahedral interstices (it is possible that octahedral sites are also occupied but this could not be determined). This diffusion is somewhat equivalent to the formation of the spinel CoAl_2O_4 from CoO and Al_2O_3 but the reaction remains far from complete. Already at a ratio $\text{Co/Al} = 0.03$ further diffusion stops and Co_3O_4 remains present as evidenced by its conversion to the metal after reduction. The diffusion into and conversion of the $\gamma\text{-Al}_2\text{O}_3$ to the pseudo-spinel is therefore apparently confined to the outer layers of the alumina particles. The excess Co_3O_4 is converted by $\text{H}_2 + \text{H}_2\text{S}$ treatment to a mixture of Co and CoS , the latter compound after a subsequent hydrogen treatment giving rise to the formation of what is either Co^{2+} or low spin Co^{2+} .

Impregnation with NH_4 molybdate and subsequent firing appears to form MoO_3 with properties which are not different from the pure compound, since just as for pure MoO_3 calcining leads to some dissociation of O_2 and the formation of small quantities of Mo^{5+} . Subsequent further reduction by H_2 and H_2S initially forms more Mo^{5+} , some of which is situated in the interior of the crystals because it does not interact with air at room temperature. Prolonged interaction with the $\text{H}_2 + \text{H}_2\text{S}$ mixture eliminates the Mo^{5+} , presumably because of a reduction to Mo^{4+} . No signal is observed that might correspond to the W^{3+} signals reported by Voorhoeve and Stuiver (9) for WS_2 . In view of van den Berg's observation (20) of the existence of diamagnetic pairs of Mo^{3+} the absence of an ESR signal cannot be considered as a proof for the absence of Mo^{3+} .

The impregnation of Co nitrate "on top" of Mo oxide presents some interesting features. First, the formation of Co metal and therefore presumably also of its precursor Co_3O_4 is entirely impeded. This might be explained by a reaction of Co oxide with Mo oxide to form a Co molybdate. At relatively low Co concentrations (3 atomic%), however, this cation is still found to be present in the alumina. Even so, its presence appears to alter the be-

havior of the MoO_3 , eliminating its tendency to form Mo^{5+} . Work by Dufaux, Che, and Naccache (21) might be relevant in this connection. They found that the intensity of the Mo^{5+} signal is strictly proportional to the amount of MoO_3 on $\gamma\text{-Al}_2\text{O}_3$ but that on $\gamma\text{-Al}_2\text{O}_3$ no signal is observed below 10% MoO_3 . They suggest that the inactive MoO_3 is present as a monolayer on the support, a similar model as given by Lipsch and Schuit (4). Now, $\text{A-}\gamma\text{-Mo-5}$ is equivalent to 14.4% MoO_3 and our observation of a weak signal is therefore in agreement with that of Dufaux *et al.* Its disappearance in the presence of Co can be explained by the reaction of the excess MoO_3 with for instance Co_3O_4 to give CoMoO_4 . The observation that the Co I signal is now stronger then leads to the suggestion that this CoMoO_4 becomes incorporated in the alumina, i.e., Co and Mo dissolve simultaneously in the support. The ESR inertness of the first amounts of MoO_3 might then also be ascribed to a solution of the Mo in the support. Hence, both Co and Mo dissolve in the alumina and in both cases the solubility is restricted. However, once they are present simultaneously their solubilities increase. This model is supported by the observations regarding the intensity of the Co IV signal. Co without Mo produces a stronger signal than when Mo is present. Contrary hereto, Hagenbach *et al.* find the signal strength in mixtures of $\text{Co}_9\text{S}_8 + \text{MoS}_2$ to be maximum at Co/Mo ratios around 0.5. An explanation for this discrepancy might be that there is less Co sulfide present when Mo is also present which means that more Co has then become dissolved in the carrier.

Obviously, since Co IV signals are observed at high Co and Mo concentrations and because of our assumption that these signals are connected with CoS (or Co_9S_8) + MoS_2 or CoMo_2S_4 , this means that the presence of these phases at high concentrations of catalyst and promoter will have to be accepted anyhow.

The combined evidence of the measurements in the oxidized and sulfided states now appears to make attractive a model in which both Co and Mo are present in the

subsurface layers of the support. The question is now whether this state reacts with H_2 or $H_2 + H_2S$ and if so, how it reacts. It has already been shown that Co^{2+} in this position is not reducible. The behavior of the Mo^{5+} (Mo I) signal during the pretreatment with $H_2 + H_2S$ in the absence and the presence of Co suggests that Mo in the support either is not reduced at all or that a reduction of the Mo^{6+} occurs that does not pass via Mo^{5+} . Whether sulfidation of these sub-surface layers occurs remains uncertain from the present measurements.

In summarizing our conclusions, we propose that the $Co-Mo$ catalyst is characterized by two solid states, viz. (I) the support with Co and Mo present in its subsurface layers, and (II) a separate compound in the pores, MoO_3 or $CoMoO_4$. Reduction and presulfiding converts II into either a mixture of $Co_9S_8 + MoS_2$ (Hagenbach *et al.*) or $CoMo_2S_4$ (van den Berg, Hagenbach *et al.*). The Co in state I is not reduced, the Mo may be so but not via Mo^{5+} : whether the subsurface layers are (partially) sulfided remains unknown.

ACKNOWLEDGMENT

One of us (M.L.) wishes to thank the Italian C.N.R. Centro di Studio on "Struttura ed Attività Catalitica di Sistemi di Ossidi," University of Rome, for a grant that enabled him to spend the academic year 1970-1971 at Eindhoven.

REFERENCES

1. RICHARDSON, J. T., *Ind. Eng. Chem. Fundamentals* **3**, 154 (1964).
2. TOMLINSON, J. R., KEELING, R. O., RYMER, G. T., AND BRIDGES, J. M., "Actes du 2me Congres International de Catalyse," Editions Technip, Paris, 1961.
3. ASHLEY, J. H., AND MITCHELL, P. C. H., *J. Chem. Soc. (A)* **2821** (1968); **2730** (1969).
4. LIPSCH, J. M. J. G., AND SCHUIT, G. C. A., *J. Catal.* **15**, 163, 174 (1969).
5. SESHADRI, K. S., AND PETRAKIS, L., *J. Phys. Chem.* **74**, 4102 (1970).
6. SESHADRI, K. S., MASSOTH, F. E., AND PETRAKIS, L., *J. Catal.* **19**, 95 (1970).
7. HAGENBACH, G., MENGUY, P., AND DELMON, B., *C. R. Acad. Sci. Paris* **273**, 1220 (1971).
8. HAGENBACH, G., COURTY, PH., AND DELMON, B., *J. Catal.* **23**, 295 (1971).
9. VOORHOEVE, R. J. H., AND STUIVER, J. C. M., *J. Catal.* **23**, 228, 236, 243 (1971).
10. McIVER, D. S., TOBIN, H. H., AND BERTH, R. T., *J. Catal.* **2**, 485 (1963).
11. MASSON, J., AND NECHTSCHHEIN, L., *Bull. Soc. Chim. Fr.* 3993 (1968).
12. DUDZIK, Z., AND PRESTON, K. F., *J. Colloid Interface Sci.* **26**, 374 (1968).
13. LOJACONO, M., VERBEEK, J. L., AND SCHUIT, G. C. A., "Proc. 5th International Congress on Catalysis," Palm Beach, Florida U.S.A. (1972), in press.
14. VAN REIJEN, L. L., Doctoral Thesis, University of Technology, Eindhoven, The Netherlands (1964).
15. SCHULZ-DUBOIS, E. O., *Bell System Techn. J.* **38**, 271 (1959).
16. ABRAGAM, A., AND BLEANEY, B., "Electron Paramagnetic Resonance," Clarendon Press, Oxford, 1970.
17. KEELING, R. O., *J. Chem. Phys.* **31**, 279 (1959).
18. LOCHER, P. R., AND GESCHWIND, S., *Phys. Rev. Lett.* **11**, 333 (1963).
19. LOW, W., AND SUSS, J. T., *Phys. Rev. Lett.* **15**, 519 (1965).
20. VAN DEN BERG, J. M., *Inorg. Chim. Acta* **2**, 216 (1968).
21. DUFAUX, M., CHE, M., AND NACCACHE, CL., *J. Chim. Phys.* **67**, 527 (1970).